American Mineralogist, Volume 97, pages 1187–1192, 2012

Reynoldsite, $Pb_2Mn^{4+}_2O_5(CrO_4)$, a new phyllomanganate-chromate from the Blue Bell claims, California and the Red Lead mine, Tasmania

ANTHONY R. KAMPF,[1,*] STUART J. MILLS,[2] ROBERT M. HOUSLEY,[3] RALPH S. BOTTRILL,[4] AND UWE KOLITSCH[5,6]

[1]Mineral Sciences Department, Natural History Museum of Los Angeles County, 900 Exposition Boulevard, Los Angeles, California 90007, U.S.A.
[2]Geosciences, Museum Victoria, GPO Box 666, Melbourne 3001, Victoria, Australia
[3]Division of Geological and Planetary Sciences, California Institute of Technology, Pasadena, California 91125, U.S.A.
[4]Mineral Resources Tasmania, P.O. Box 56, Rosny Park, Tasmania 7018, Australia
[5]Mineralogisch-Petrographische Abt., Naturhistorisches Museum, Burgring 7, A-1010 Wien, Austria
[6]Institut für Mineralogie und Kristallographie, Universität Wien, Geozentrum, Althanstrasse 14, A-1090 Wien, Austria

ABSTRACT

The new mineral reynoldsite, $Pb_2Mn^{4+}_2O_5(CrO_4)$, occurs at the Blue Bell claims, near Baker, San Bernardino County, California, U.S.A., and at the Red Lead mine, Dundas, Tasmania, Australia. At the Blue Bell claims, reynoldsite occurs in subparallel growths and divergent sprays of thin prisms with a square cross section. At the Red Lead mine, it occurs as thin rectangular blades. At both occurrences, crystals are small (≤0.2 mm), and ubiquitously and multiply twinned. At both deposits, reynoldsite formed as a secondary mineral derived from the weathering of primary minerals including oxides and sulfides in the presence of acidic groundwater. Reynoldsite is dark orange-brown to black in color and has a dark orange-brown streak. Its luster is subadamantine and its Mohs hardness is about 4½. The mineral is brittle with irregular to splintery fracture and a poorly developed {001} cleavage. The calculated density is 6.574 g/cm^3 (Red Lead mine). The very high indices of refraction and dark color permitted only partial determination of the transmitted light optical properties. Electron microprobe analyses of Blue Bell and Red Lead reynoldsite provided the empirical formulas (based on nine O atoms): $Pb_{1.97}Mn_{2.01}O_5(Cr_{1.01}O_4)$ and $(Pb_{2.07}Sr_{0.04})_{\Sigma 2.11}Mn_{2.15}O_5(Cr_{0.87}O_4)$, respectively. The strongest powder X-ray diffraction lines for Red Lead reynoldsite are [$d(hkl)I$]: 3.427($0\bar{2}1$,110)52, 3.254(021,$1\bar{1}2$,$1\bar{2}1$)85, 3.052($\bar{1}\bar{1}2$,111,$0\bar{2}2$,$\bar{1}03$)100, 2.923(013,$\bar{1}22$)40, 2.5015(004,$\bar{2}11$,$\bar{1}30$)47, 1.9818($0\bar{1}5$,$\bar{1}05$,202,$2\bar{3}1$)42, 1.7694($1\bar{1}5$,$1\bar{3}4$,203,$\bar{1}42$,$\bar{1}\bar{3}3$)36, and 1.6368($\bar{2}\bar{2}3$,$0\bar{4}3$,221,124,$2\bar{2}4$)36. Reynoldsite is triclinic with space group $P\bar{1}$ and unit-cell parameters: $a = 5.0278(7)$, $b = 7.5865(11)$, $c = 10.2808(15)$ Å, $\alpha = 91.968(12)$, $\beta = 99.405(12)$, $\gamma = 109.159(10)°$, $V = 363.81(9)$ Å^3, and $Z = 2$ (for a Red Lead mine crystal). The crystal structure of reynoldsite ($R_1 = 10.2\%$ for 902 reflections with $F_o > 4\sigma F$ for a Red Lead crystal) contains close-packed layers of edge-sharing $Mn^{4+}O_6$ octahedra parallel to {001}. These layers are composed of edge-sharing double chains of octahedra extending along [100], which in turn are linked to one another by sharing edges in the [010] direction. The thick interlayer region contains Pb^{2+} cations and CrO_4 tetrahedra. The 6s^2 lone-electron pair of the Pb^{2+} is stereochemically active, resulting in a one-sided Pb-O coordination arrangement. The structure bears strong similarities to those of the phyllomanganates, such as chalcophanite and birnessite.

Keywords: Reynoldsite, new mineral, crystal structure, phyllomanganate, chromate, Pb^{2+} 6s^2 lone-electron pair, Blue Bell claims, California, Red Lead mine, Tasmania

INTRODUCTION

The new mineral described herein was first noted as occurring at the Red Lead mine, Dundas, Tasmania, Australia, by Bottrill et al. (2006) and was listed as valid unnamed mineral UM2006-04 by Smith and Nickel (2007). In 2009, the mineral was found by collectors Joseph Marty and Brent Thorne at the Blue Bell claims near Baker, San Bernardino County, California, U.S.A., and they provided specimens for study.

The name is in honor of Robert E. Reynolds (b. 1943), former Curator of Earth Sciences at the San Bernardino County Museum. Influential instructors at Pasadena City College (Pasadena, California) and the University of California, Riverside, inspired R.E. Reynolds to pursue mineralogical and paleontological studies of the Mojave Desert and he has maintained this focus for more than four decades. He has written or edited numerous publications and has organized many symposia focused on the Mojave Desert region. Over the course of several years, he coordinated and supported a dedicated group of volunteers from the San Bernardino County Museum in an extensive study of the Blue Bell claims, which culminated in a publication detailing the history and mineralogy of the deposit (Maynard et al. 1984).

The new mineral and name have been approved by the Commission on New Minerals, Nomenclature and Classification of the International Mineralogical Association (IMA 2011-051).

---

* E-mail: akampf@nhm.org

0003-004X/12/0007–1187$05.00/DOI: http://dx.doi.org/10.2138/am.2012.3989

There is no specimen that qualifies as the holotype; however, four cotype specimens are deposited in the Natural History Museum of Los Angeles County under catalog numbers 63559, 63560, and 63561 (Blue Bell claims) and 63562 (Red Lead mine).

OCCURRENCE

The mineral occurs at the Blue Bell claims in the Soda Mountains about 11 km west of Baker, San Bernardino County, California, U.S.A. (35°14′3″N 116°12′17″W) (Crowley 1977; Maynard et al. 1984) and at the Red Lead mine, Dundas, Tasmania, Australia (41°53′22″S 145°25′51″E) (Bottrill et al. 2006); both are considered type localities. The new mineral has also been confirmed to occur at the Milford no.3 mine, Goodsprings district, Nevada, U.S.A., but material from this occurrence has not been used in the description of the species.

At the Blue Bell claims, reynoldsite occurs in an adit, referred to as the C adit, in cracks and very narrow veins in a highly siliceous hornfels. Species observed in direct association with the new mineral include: coronadite, fluorite, goethite, opal, pyromorphite, quartz, and wulfenite. Other species identified in the same general assemblage include beudantite, boleite, calcite, celestine, cerussite, chrysocolla, creaseyite, dioptase, ferrisurite, fluorapatite, fluorphosphohedyphane (Kampf and Housley 2011), gypsum, hemimorphite, mimetite, mottramite, phosphohedyphane, plumbogummite, plumbophyllite (Kampf et al. 2009), plumbotsumite, and vanadinite. At the Red Lead mine, reynoldsite occurs coating stalactitic coronadite and lithiophorite, and is locally overgrown by crocoite crystals (Bottrill and Baker 2008). The samples were not observed in situ, but were apparently extracted from some erratic plumbiferous veins that are locally manganiferous, in an open pit dug for crocoite (for which the mine is operated commercially). Other minerals found in the gossans of this mine include: anglesite, cerussite, chalcophanite, dundasite, goethite, grimaldiite, petterdite, philipsbornite, and pyrolusite (Bottrill et al. 2006).

The Blue Bell claims exploit the oxidation zone of a small Pb-Cu-Zn-Ag deposit, while the Red Lead mine exploits a supergene mineral assemblage, which has resulted from the superposition of carbonate-altered, Cr-rich, ultramafic rocks (containing stichtite, "fuchsite," and magnesiochromite) with galena-rich veins, followed by deep weathering by acid groundwater (Bottrill et al. 2006). At both localities reynoldsite formed as a secondary mineral derived from the weathering of primary minerals including oxides and sulfides in the presence of acidic groundwater.

PHYSICAL AND OPTICAL PROPERTIES

At the Blue Bell claims reynoldsite occurs as thin prisms, elongated parallel to [100] with a square cross section and a chisel-like termination. Prisms are up to 0.2 mm long and 0.02 mm in diameter, display the forms {010}, {001}, {102}, and {10$\overline{2}$}, and are grouped into subparallel growths and divergent sprays. At the Red Lead mine reynoldsite occurs as thin rectangular blades, flattened on {001} and elongated parallel to [100] and commonly curved (Fig. 1). Crystals are up to 0.1 mm in length and display the forms {001} and {010}. At both occurrences, crystals exhibit ubiquitous multiple penetration and reticulated twinning by rotations on [100] and [120] and about the normal to {001}. At the Blue Bell claims multiple twinning is sometimes manifest as small "arms" projecting from larger crystals (Fig. 2). At the Red Lead mine multiple twinning is sometimes manifested in pseudohexagonal platelets.

The mineral is dark orange-brown to black. The orange-brown color is only seen in very thin crystals in strong transmitted light. The streak is dark orange-brown and the luster is adamantine. The Mohs' hardness is about 4½. The tenacity is brittle, the fracture is irregular to splintery, and there is one cleavage parallel to {001}, which is poorly developed, probably because of the pervasive multiple penetration twinning. The mineral is non-fluorescent in SW and LW ultraviolet light. The density could not be measured because it is greater than available high-density liquids and there is insufficient material for physical measurement. The density calculated based on the ideal formula and Red Lead mine single-crystal unit cell is 6.574 g/cm^3.

The optical properties could not be fully determined because

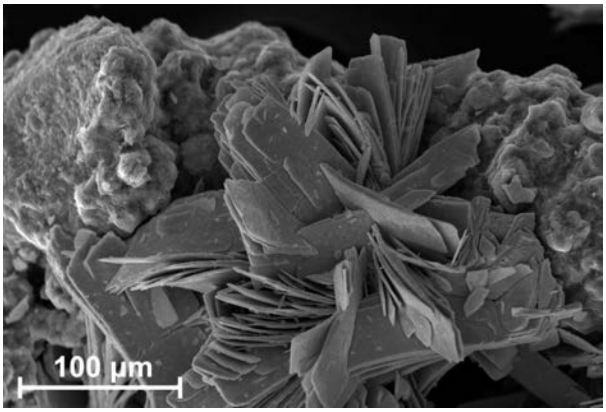

FIGURE 1. SEM image of curved reynoldsite plates/blades from the Red Lead mine.

FIGURE 2. Multiply twinned crystal of reynoldsite from the Blue Bell claims (0.1 mm tall); plane-polarized light micrograph. (Color online.)

of the small size of the crystals, the high indices of refraction, the dark color, and the twinning. The Gladstone-Dale relationship (Mandarino 1981) predicts $n_{av} = 2.473$ based upon for the ideal formula. The mineral is biaxial based on its crystal symmetry. Extinction is approximately parallel to [100], the direction of prism elongation for Blue Bell crystals and of the plate edges of Red Lead crystals. Very thin plates exhibit an orange-brown color in transmitted light and are pleochroic from medium brown along [100] to dark orange-brown along [010]*.

CHEMISTRY

Two chemical analyses on Blue Bell reynoldsite were carried out using a JEOL8200 electron microprobe in the Division of Geological and Planetary Sciences, California Institute of Technology (WDS mode, 15 kV and 5 nA focused beam) with the standards galena (Pb), Mn-olivine (Mn), and crocoite (Cr). Two chemical analyses on Red Lead reynoldsite were carried out using a Cameca SX50 electron microprobe in the Central Science Laboratories, University of Tasmania (WDS mode, 15 kV, 25 nA, and 10 μm beam) with the standards NBS624 (Pb), celestine (Sr), rhodonite (Mn), and chromite (Cr). Note that the crystal structure analyses indicate reynoldsite to be anhydrous, so the low totals may be attributed to the difficulty in analyzing the small, thin crystals, rather than to the presence of OH and/or H_2O. Note that for the Blue Bell reynoldsite analyses, the surface of the best grain measured only 3.5 × 6.5 μm. For Blue Bell reynoldsite, no other elements were detected by EDS, and in the microprobe analyses Al, Si, Cl, S, Ca, Fe, Cu, As, and Te were below detection limits. For Red Lead reynoldsite, traces of Na, Ba, Ca, Co, Cu, Zn, Al, and As were noted, but were below the microprobe detection limits. Analytical averages (with individual analyses in parentheses) for Blue Bell material are: PbO (58.54, 59.27) 58.90, MnO_2 (23.06, 23.61) 23.34, CrO_3 (13.40, 13.53) 13.46, total 95.70 wt%; for Red Lead mine material are: PbO (60.47, 61.11) 60.79, SrO (0.50, 0.52) 0.51, MnO_2 (24.58, 24.67) 24.63, CrO_3 (11.39, 11.41) 11.40, total 97.33 wt%. The empirical formulas (based on nine O atoms) for Blue Bell and Red Lead reynoldsite are: $Pb_{1.97}Mn_{2.01}O_5(Cr_{1.01}O_4)$ and $(Pb_{2.07}Sr_{0.04})_{\Sigma 2.11}Mn_{2.15}O_5(Cr_{0.87}O_4)$, respectively. Reynoldsite dissolves slowly in concentrated HCl.

X-RAY CRYSTALLOGRAPHY AND STRUCTURE DETERMINATION

Both powder and single-crystal X-ray diffraction data were obtained on a Rigaku R-Axis Rapid II curved imaging plate microdiffractometer utilizing monochromatized Mo$K\alpha$ radiation. The powder data presented in Table 1 show good agreement with the pattern calculated from the structure determination.

TABLE 1. Powder data for reynoldsite (Red Lead mine)*

I_{obs}	d_{obs}	d_{calc}	I_{calc}	$h\,k\,l$
5	5.61(2)	5.5835	11	0 1 1
2	5.076(17)	5.0487	19	0 0 2
26	4.710(4)	4.7027	59	$\bar{1}$ 1 0
26	4.60(2)	4.5710	18	$\bar{1}$ 0 1
11	3.944(6)	3.9491	23	0 1 2
16	3.676(3)	3.6764	33	$\bar{1}$ 1 2
52	3.427(3)	3.4678	43	0 $\bar{2}$ 1
		3.4255	7	$\bar{1}$ $\bar{1}$ 1
		3.4122	39	1 1 0
		3.3658	29	0 0 3
		3.3146	27	$\bar{1}$ 2 1
85	3.2536(15)	3.2679	26	0 2 1
		3.2459	100	1 $\bar{1}$ 2
		3.2234	17	1 $\bar{2}$ 1
100	3.0517(12)	3.0983	25	$\bar{1}$ $\bar{1}$ 2
		3.0690	65	1 $\bar{1}$ 1
		3.0523	60	0 $\bar{2}$ 2
		3.0066	60	$\bar{1}$ 0 3
40	2.9228(19)	2.9389	18	0 1 3
		2.9131	49	$\bar{1}$ 2 2
2	2.785(6)	2.7918	8	0 2 2
5	2.608(3)	2.6165	4	1 1 2
		2.5890	7	1 $\bar{1}$ 3
		2.5723	5	0 $\bar{2}$ 3
47	2.5015(4)	2.5243	8	0 0 4
		2.5053	51	$\bar{2}$ 1 1
		2.4866	10	$\bar{1}$ 3 0
30	2.374(2)	2.4152	6	$\bar{1}$ 0 4
		2.4146	11	1 $\bar{3}$ 1
		2.3781	15	0 3 0
		2.3688	10	$\bar{1}$ $\bar{2}$ 2
19	2.314(2)	2.3121	26	0 1 4
9	2.2304(15)	2.2309	15	$\bar{1}$ $\bar{1}$ 4
		2.2306	6	$\bar{1}$ 3 2
28	2.1794(10)	2.1867	13	2 0 1
		2.1738	13	$\bar{2}$ 1 3
		2.1589	15	0 $\bar{2}$ 4
19	2.0841(9)	2.0943	8	2 $\bar{1}$ 2
		2.0837	15	$\bar{1}$ 2 4
		2.0771	19	0 3 2
18	2.0498(16)	2.0479	13	$\bar{2}$ 3 0
		2.0369	10	2 $\bar{2}$ 2
42	1.9818(12)	1.9930	12	0 $\bar{1}$ 5
		1.9927	6	$\bar{1}$ 0 5
		1.9832	6	2 0 2
		1.9761	17	2 $\bar{3}$ 1
24	1.8964(3)	1.8992	14	$\bar{2}$ $\bar{1}$ 3
		1.8972	19	$\bar{1}$ $\bar{3}$ 1
		1.8935	15	$\bar{1}$ 4 0
12	1.857(2)	1.8612	4	0 3 3
		1.8565	5	2 $\bar{1}$ 3
36	1.7694(6)	1.7773	6	1 $\bar{1}$ 5
		1.7716	20	1 $\bar{3}$ 4
		1.7705	11	2 0 3
		1.7584	9	$\bar{1}$ 4 2
		1.7545	9	$\bar{1}$ $\bar{3}$ 3
23	1.7056(9)	1.7090	11	$\bar{2}$ 1 5
		1.7028	21	$\bar{1}$ $\bar{2}$ 5
36	1.6368(5)	1.6463	6	$\bar{2}$ $\bar{2}$ 3
		1.6414	12	0 $\bar{4}$ 3
		1.6345	10	2 2 1
		1.6341	15	1 2 4
		1.6229	8	2 $\bar{2}$ 4
34	1.5744(7)	1.5861	5	$\bar{2}$ $\bar{1}$ 5
		1.5854	11	3 $\bar{2}$ 1
		1.5751	7	$\bar{3}$ 2 3
		1.5675	7	$\bar{1}$ 3 5
		1.5657	5	$\bar{2}$ 4 3
10	1.4982(8)	1.4991	4	$\bar{3}$ 1 4
		1.4972	7	1 0 6
21	1.4428(5)	1.4473	5	$\bar{3}$ $\bar{1}$ 1
		1.4458	5	2 $\bar{2}$ 5
		1.4430	6	$\bar{3}$ 4 1
		1.4382	6	$\bar{3}$ 4 0
17	1.4009(11)	1.4065	5	$\bar{2}$ 5 2
		1.4039	4	2 0 5
		1.3923	5	2 $\bar{5}$ 2

* Calculated lines of intensity less than 12 are listed only if they contribute to observed lines. Calculated lines for 003 and $\bar{1}21$ are contained in the shoulder of the observed 3.427 Å line.

The Rigaku CrystalClear software package and specifically the TwinSolve program was used for processing of the single-crystal data. The SHELXL-97 software (Sheldrick 2008) was used for the solution and refinement of the structure. The very small size and ubiquitous multiple twinning of reynoldsite crystals made the solution of the crystal structure highly challenging. After countless failed attempts to find a suitable crystal, we finally found a 25 × 4 × 2 μm^3 crystal from the Blue Bell claims that consisted of only two well-defined twin components related by 180° rotation about [120]. The data obtained from both twin components of this crystal allowed the solution of the structure. We later succeeded in finding a 25 × 20 × 1 μm^3 crystal from the Red Lead mine consisting of two twin components related by 180° rotation about the normal to {001}. The data obtained from both twin components of that crystal provided a better refinement, the results of which are presented herein. Because of the necessity of using a twinned crystal, only an empirical absorption correction was applied. The twinning and the very small size of the crystal resulted in a limited data set of relatively poor quality. For this reason, the atom displacement parameters could not be refined anisotropically and isotropic displacement parameters for O5, O6, and O8 refined to anomalously low values. In the final refinement, the isotropic displacement parameters for these three atoms were therefore set to 0.015 Å^2.

The chemical analyses of Red Lead reynoldsite provided a small amount of Sr. We attempted to refine the Pb sites with joint occupancy by Pb and Sr; however, this resulted in an only slightly improved refinement ($R_1 = 0.1014$ vs. 0.1016), so in the final refinement we elected to assign full occupancy by Pb to both Pb sites. High (and low) electron density residuals are further indication of the relatively poor quality of the data. Difference Fourier synthesis provided 16 peaks <2.0 e/A^3. All but one of these is in the layer portion of the structure; however, attempts to refine the displacement parameters of the cations anisotropically failed to significantly diminish the electron density residuals, provided unreasonable ellipsoids for all except Pb2 and did not substantially reduce R_1 (0.0987 vs. 0.1016).

The details of the data collection and structure refinement are provided in Table 2. The final atomic coordinates and displacement parameters are in Table 3. Selected interatomic distances are listed in Table 4 and bond valences in Table 5. (CIF and structure factor table are available[1].)

DESCRIPTION OF THE STRUCTURE

The crystal structure of reynoldsite (Fig. 3) contains close-packed layers of edge-sharing Mn^{4+}O$_6$ octahedra parallel to {001}. These layers are composed of edge-sharing double chains of octahedra extending along [100], which in turn are linked to one another by sharing edges in the [010] direction. The thick interlayer region contains Pb^{2+} cations and CrO$_4^{2-}$ tetrahedra. Both

TABLE 2. Data collection and structure refinement details for reynoldsite (Red Lead mine)

Diffractometer	Rigaku R-Axis Rapid II	
X-ray radiation/power	Mo$K\alpha$ ($\lambda = 0.71075$ Å)/50 kV, 40 mA	
Temperature	298(2) K	
Structural formula	Pb$_2$Mn$^{4+}_2$O$_5$(CrO$_4$)	
Space group	$P\overline{1}$	
Unit-cell dimensions	$a = 5.0278(7)$ Å	$\alpha = 91.968(12)°$
	$b = 7.5865(11)$ Å	$\beta = 99.405(12)°$
	$c = 10.2808(15)$ Å	$\gamma = 109.159(10)°$
Z	2	
Volume	363.81(9) Å^3	
Density (for formula above)	6.575 g/cm^3	
Absorption coefficient	50.967 mm^{-1}	
F(000)	626	
Crystal size	25 × 20 × 1 μm^3	
θ range	2.0 to 20.02°	
Max. and min. transmission	0.9508 and 0.3623	
Index ranges	$0 \leq h \leq 4, -7 \leq k \leq 6, -9 \leq l \leq 9$	
Reflections collected/unique	1251/1251	
Reflections with $F_o > 4\sigma F$	902	
Completeness to θ = 20.02°	98.1%	
Refinement method	Full-matrix least-squares on F^2	
Parameters refined	56	
GoF	1.156	
Final R indices [$F_o > 4\sigma F$]	$R_1 = 0.1016$, w$R_2 = 0.2118$	
R indices (all data)	$R_1 = 0.1407$, w$R_2 = 0.2277$	
Extinction coefficient	0.010(2)	
Largest diff. peak/hole	+3.2/–3.0 e/A^3	
Twin component proportions	0.642(4)/0.358(4)	

Notes: GoF = $S = \{\Sigma[w(F_o^2 - F_c^2)^2]/(n-p)\}^{1/2}$. $R_1 = \Sigma||F_o| - |F_c||/\Sigma|F_o|$. $wR_2 = \{\Sigma[w(F_o^2 - F_c^2)^2]/\Sigma[w(F_o^2)^2]\}^{1/2}$. $w = 1/[\sigma^2(F_o^2) + (aP)^2 + bP]$ where a is 0.1034, b is 28.2146, and P is $[2F_c^2 + \mathrm{Max}(F_o^2,0)]/3$.

TABLE 3. Atom coordinates and isotropic displacement parameters (Å^2) for reynoldsite (Red Lead mine)

	x/a	y/b	z/c	U_{iso}
Pb1	0.1082(5)	0.0396(3)	0.7436(3)	0.0161(11)
Pb2	0.5013(6)	0.6126(4)	0.8184(3)	0.0260(12)
Mn1	0.6008(19)	0.1968(12)	0.5028(10)	0.009(2)
Mn2	0.1950(18)	0.3944(12)	0.4931(10)	0.015(3)
Cr	0.807(2)	0.2354(14)	0.9544(11)	0.015(2)
O1	0.554(8)	0.325(5)	0.929(4)	0.012(10)
O2	0.053(8)	0.349(5)	0.869(4)	0.016(11)
O3	0.953(9)	0.267(6)	0.114(5)	0.026(12)
O4	0.689(9)	0.009(6)	0.886(5)	0.027(12)
O5	0.830(8)	0.384(5)	0.402(4)	0.015*
O6	0.436(8)	0.588(5)	0.401(4)	0.015*
O7	0.420(9)	0.006(6)	0.605(4)	0.023(12)
O8	0.255(9)	0.218(6)	0.390(4)	0.015*
O9	0.989(8)	0.235(5)	0.597(4)	0.011(10)

* Fixed.

TABLE 4. Selected bond distances (Å) in reynoldsite (Red Lead mine)

Pb1-O9	2.30(4)	Pb2-O3	2.56(4)	Mn1-O7	1.83(4)	Mn2-O8	1.81(4)	Cr-O1	1.62(4)
Pb1-O7	2.35(4)	Pb2-O1	2.57(4)	Mn1-O7	1.89(4)	Mn2-O9	1.82(4)	Cr-O2	1.66(5)
Pb1-O8	2.38(4)	Pb2-O5	2.59(4)	Mn1-O9	1.96(4)	Mn2-O5	1.89(4)	Cr-O3	1.66(4)
Pb1-O4	2.71(4)	Pb2-O2	2.62(4)	Mn1-O6	1.96(4)	Mn2-O6	1.95(4)	Cr-O4	1.71(4)
Pb1-O3	2.75(4)	Pb2-O1	2.70(4)	Mn1-O5	1.96(4)	Mn2-O6	1.95(4)	<Cr-O>	1.66
Pb1-O2	2.75(4)	Pb2-O8	2.78(4)	Mn1-O8	1.99(4)	Mn2-O5	2.02(4)		
Pb1-O1	2.91(4)	Pb2-O6	2.79(4)	<Mn-O>	1.95	<Mn-O>	1.92		
Pb1-O4	3.13(5)	Pb2-O4	2.86(4)						
<Pb-O>	2.66	Pb2-O3	2.89(4)						
		<Pb-O>	2.71						

---

[1] Deposit item AM-12-061, Structure factor table and CIF. Deposit items are available two ways: For a paper copy contact the Business Office of the Mineralogical Society of America (see inside front cover of recent issue) for price information. For an electronic copy visit the MSA web site at http://www.minsocam.org, go to the *American Mineralogist* Contents, find the table of contents for the specific volume/issue wanted, and then click on the deposit link there.

TABLE 5. Bond-valence analysis for reynoldsite (Red Lead mine)

	O1	O2	O3	O4	O5	O6	O7	O8	O9	Σ
Pb1	0.14	0.20	0.20	0.22, 0.09			0.45	0.43	0.50	2.23
Pb2	0.29, 0.22	0.26	0.30, 0.15	0.16	0.28	0.18		0.19		2.03
Mn1					0.57	0.57	0.81, 0.69	0.53	0.57	3.74
Mn2					0.69, 0.49	0.59, 0.59		0.86	0.83	4.05
Cr	1.60	1.44	1.44	1.25						5.73
Σ	2.25	1.90	2.09	1.72	2.03	1.93	1.95	2.01	1.90	

Notes: Values are expressed in valence units. Pb^{2+}-O bond strengths from Krivovichev and Brown (2001); Mn^{4+}-O and Cr^{6+}-O bond strengths from Brown and Altermatt (1985).

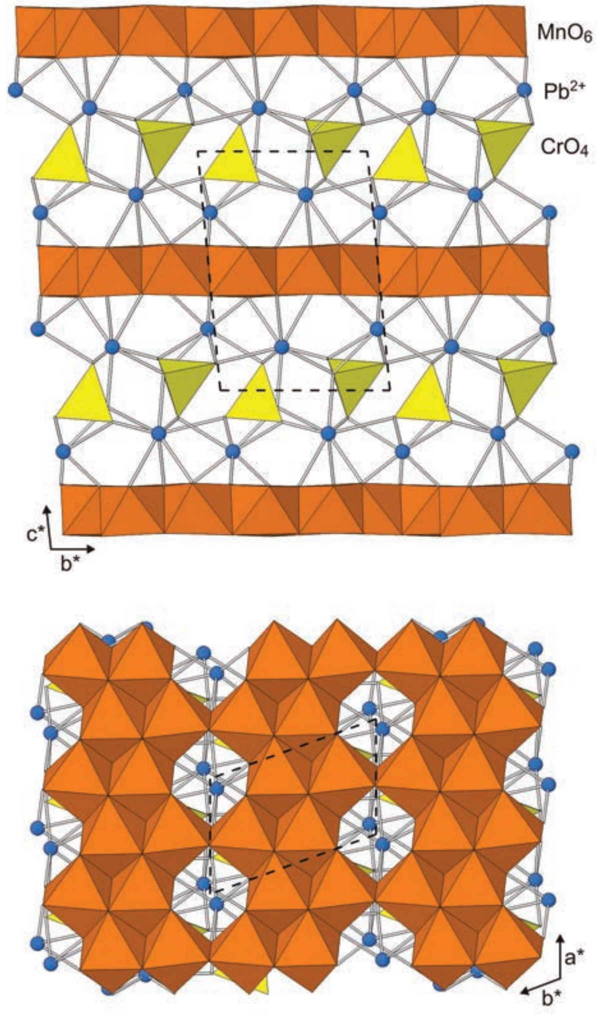

FIGURE 3. The crystal structure of reynoldsite. The unit cell is shown with dashed lines. (Color online.)

Pb^{2+} cations exhibit asymmetric coordination spheres typical of this cation with a stereochemically active $6s^2$ lone-electron pair, although the asymmetry is more pronounced for Pb1, as is reflected in the larger range of Pb1-O bond lengths.

Despite the poor quality of the data and the high-*R* factor, the details of the structure are quite reasonable. The $Mn^{4+}O_6$ octahedra are significantly distorted, but no more so than in some similar structures, and the average Mn-O bond lengths are well within normal limits. For example, for coronadite Post and Bish (1989) report Mn-O bond lengths in one $Mn^{4+}O_6$ octahedron from 1.79 to 2.02 Å with <Mn-O> = 1.90 Å. For chalcophanite, Post and Appleman (1988) report bond lengths from 1.857 to 1.967 Å with <Mn-O> = 1.906 Å. In a study on the crystal structure of synthetic birnessite, Post and Veblen (1990) suggest that the average Mn-O bond lengths of 1.93 and 1.94 Å, being higher than that reported for chalcophanite, may result from a small amount of Mn^{3+} substituting for Mn^{4+}. This also seems to fit the Mn1 site in reynoldsite, for which <Mn-O> = 1.95 Å and the bond-valence sum (BVS) is 3.75 v.u.

The geometry of the CrO_4 tetrahedron is also quite reasonable (O-Cr-O angles range from 104 to 115°) and, although the range of Cr-O bond lengths is fairly large (1.62 to 1.71 Å), this is relatively common in chromates and the average Cr-O bond length, 1.66 Å, is within normal limits. As examples, the CrO_4 tetrahedron in edoylerite (Burns 1999) has Cr-O bond lengths ranging from 1.60 to 1.69 Å with <Cr-O> = 1.64 Å, and in hemihedrite (McLean and Anthony 1970) the three tetrahedra have the ranges (and averages): 1.64–1.68 (1.66), 1.60–1.69 (1.66), and 1.60–1.70 (1.66 Å). The Cr-O bond length has a very strong effect on the BVS of the corresponding O atom. We observe in reynoldsite that the O1 atom participating in the unusually short Cr-O1 bond (1.62 Å) has a much higher than normal BVS (2.25 v.u.) and the O4 atom participating in the unusually long Cr-O4 bond (1.71 Å) has a much lower than normal BVS (1.72 v.u.). Similarly, in edoylerite the O atom corresponding to the short Cr-O bond (1.60 Å) has a BVS of 2.11 v.u. and the O atom corresponding to the long Cr-O bond (1.69 Å) has a BVS of 1.77 v.u. We suggest that this may reflect a need to revise the bond-valence parameters for Cr^{6+}-O bonds and that a more complete analysis of Cr^{6+}-O bonds in inorganic compounds seems warranted.

The reynoldsite structure bears strong similarities to those of phyllomanganates, such as chalcophanite, $ZnMn_3^{4+}O_7{\cdot}3H_2O$ (Post and Appleman 1988), and birnessite, $(Na,Ca,K)_{0.6}(Mn^{4+},Mn^{3+})_2O_4{\cdot}1.5H_2O$ (Post and Veblen 1990). The chalcophanite structure contains close-packed layers of edge-sharing MnO_6 octahedra with fewer and differently distributed "holes" (missing Mn^{4+} cations) than in the reynoldsite structure. Above and below the holes in the chalcophanite layers are $ZnO_3(H_2O)_3$ octahedra, which link to the layers by corner-sharing. The structure of ranciéite, $Ca_{0.19}K_{0.01}(Mn^{4+}_{0.91}\square_{0.09})O_2{\cdot}0.63H_2O$ (Post et al. 2008), a member of the birnessite family, consists of close-packed layers of edge-sharing MnO_6 octahedra, between which are Ca atoms in octahedral coordination and H_2O molecules. The Mn sites in the octahedral layers have 10% vacancies (holes) and the interlayer Ca^{2+} cations are located above and below the Mn vacancies. The most important difference between the structure of reynoldsite and those of the phyllomanganate minerals is the lack of H_2O and the presence of the CrO_4 group in the center of the interlayer region in reynoldsite. In this respect, reynoldsite can be termed a phyllomanganate-chromate.

It is also noteworthy that the allactite, $Mn^{2+}_7(AsO_4)_2(OH)_8$, structure (Moore 1968) contains the same edge-sharing double chains of octahedra as in the reynoldsite structure; however, in allactite these chains are linked into layers by sharing corners with other MnO_6 octahedra and the layers are linked to one another through AsO_4 tetrahedra.

ACKNOWLEDGMENTS

Two anonymous reviewers provided helpful comments on the manuscript. Joseph Marty of Salt Lake City, Utah, and Brent Thorne of Bountiful, Utah, are thanked for providing the Blue Bell specimens used in this study. The microprobe analyses of Blue Bell material were supported by a grant to the California Institute of Technology from the Northern California Mineralogical Association. The remainder of this study was funded by the John Jago Trelawney Endowment to the Mineral Sciences Department of the Natural History Museum of Los Angeles County. This paper is published with the approval of Kim Creak, the Director of Mines, Tasmania. The work by R.S.B. was undertaken during research for the publication a Catalog of the Minerals of Tasmania (Bottrill and Baker 2008).

REFERENCES CITED

Bottrill, R.S. and Baker, W.E. (2008) A Catalogue of the Minerals of Tasmania. Tasmanian Geological Survey Bulletin, 73, 254 pp.

Bottrill, R.S., Williams, P.A., Dohnt, S., Sorrell, S., and Kemp, N.R. (2006) Crocoite and associated minerals from Tasmania. Australian Journal of Mineralogy, 12, 59–90.

Brown, I.D. and Altermatt, D. (1985) Bond-valence parameters from a systematic analysis of the inorganic crystal structure database. Acta Crystallographica, B41, 244–247.

Burns, P.C. (1999) The structure of edoylerite determined from a microcrystal. Canadian Mineralogist, 37, 113–118.

Crowley, J.A. (1977) Minerals of the Blue Bell mine, San Bernardino County, California. Mineralogical Record, 8, 494–496 and 518.

Kampf, A.R. and Housley, R.M. (2011) Fluorphosphohedyphane, the fluorine analogue of phosphohedyphane from the Blue Bell claims near Baker, San Bernardino County, California. American Mineralogist, 96, 423–429.

Kampf, A.R., Rossman, G.R., and Housley, R.M. (2009) Plumbophyllite, a new mineral from the Blue Bell claims near Baker, San Bernardino County, California. American Mineralogist, 94, 1198–1204.

Krivovichev, S.V. and Brown, I.D. (2001) Are the compressive effects of encapsulation an artifact of the bond valence parameters? Zeitschrift für Kristallographie, 216, 245–247.

McLean, W.J. and Anthony, J.W. (1970) The crystal structure of hemihedrite. American Mineralogist, 55, 1103–1114.

Mandarino, J.A. (1981) The Gladstone-Dale relationship: Part IV. The compatibility concept and its application. Canadian Mineralogist, 19, 441–450.

Maynard, M.F., Valenti, A., Jenkins, J., Jenkins, F., Hall, D., Hall, J., White, B., White, S., Mansfield, M., and Mansfield, E. (1984) The Blue Bell Claims. San Bernardino County Museum Special Publication, San Bernardino County Museum, California, 61 pp.

Moore, P.B. (1968) Crystal chemistry of the basic manganese arsenate minerals: II. The crystal structure of allactite. American Mineralogist, 53, 733–741.

Post, J.E. and Appleman, D.E. (1988) Chalcophanite, $ZnMn_3O_7{\cdot}3H_2O$: new crystal-structure determinations. American Mineralogist, 73, 1401–1404.

Post, J.E. and Bish, D.L. (1989) Rietveld refinement of the coronadite structure. American Mineralogist, 74, 913–917.

Post, J.E. and Veblen, D.R. (1990) Crystal structure determinations of synthetic sodium, magnesium, and potassium birnessite using TEM and the Rietveld method. American Mineralogist, 75, 477–489.

Post, J.E., Heaney, P.J., and Ertl, A. (2008) Rietveld refinement of the ranciéite structure using synchrotron powder diffraction data. Powder Diffraction, 23, 10–14.

Sheldrick, G.M. (2008) A short history of SHELX. Acta Crystallographica, A64, 112–122.

Smith, D.G.W. and Nickel, E.H. (2007) A system for codification for unnamed minerals: report of the Subcommittee for Unnamed Minerals of the IMA Commission on New Minerals, Nomenclature and Classification. Canadian Mineralogist, 45, 983–1055.

MANUSCRIPT RECEIVED SEPTEMBER 1, 2011
MANUSCRIPT ACCEPTED JANUARY 1, 2012
MANUSCRIPT HANDLED BY G. DIEGO GATTA